



**HAL**  
open science

## Tracking arterial wall motion in a 2D+t volume

Guillaume Zahnd, Maciej Orkisz, Simone Balocco, André Sérusclat, Philippe Moulin, Didier Vray

► **To cite this version:**

Guillaume Zahnd, Maciej Orkisz, Simone Balocco, André Sérusclat, Philippe Moulin, et al.. Tracking arterial wall motion in a 2D+t volume. 2014 IEEE-EMBS International Conference on Biomedical and Health Informatics (BHI), Jun 2014, Valencia, Spain. 10.1109/BHI.2014.6864453 . hal-01404978

**HAL Id: hal-01404978**

**<https://hal.science/hal-01404978>**

Submitted on 30 May 2018

**HAL** is a multi-disciplinary open access archive for the deposit and dissemination of scientific research documents, whether they are published or not. The documents may come from teaching and research institutions in France or abroad, or from public or private research centers.

L'archive ouverte pluridisciplinaire **HAL**, est destinée au dépôt et à la diffusion de documents scientifiques de niveau recherche, publiés ou non, émanant des établissements d'enseignement et de recherche français ou étrangers, des laboratoires publics ou privés.

# Tracking arterial wall motion in a 2D+t volume

Guillaume Zahnd<sup>1</sup>, Maciej Orkisz<sup>2</sup>, Simone Balocco<sup>3,4</sup>, André Sérusclat<sup>5</sup>, Philippe Moulin<sup>6,7</sup>, Didier Vray<sup>2</sup>

**Abstract**—The aim of this study is to propose a motion tracking framework dedicated to estimate the trajectory of the common carotid artery wall in B-mode ultrasound sequences. As the image quality of routinely acquired scans is often degraded by a number of factors, accurate estimation of the tissues motion is a challenging task. To address this issue, the main feature of our method is the research of an optimal *a posteriori* solution, which is computed using a dynamic programming scheme once all frames have been processed. Applied *in vivo* on 15 healthy volunteers, our method showed an overall good tracking performance, with an average absolute tracking error of  $104 \pm 127 \mu\text{m}$  and  $29 \pm 57 \mu\text{m}$ , in the longitudinal and radial directions, respectively. This work has potential to improve motion estimation in ultrasound imaging, and could contribute to provide more reliable information about vascular health in a clinical setting.

## I. INTRODUCTION

Cardiovascular diseases are the primary cause of mortality worldwide [1]. Yet, cardiovascular risk prediction is challenging, as the screening potential of traditional imaging biomarkers, such as pulse wave velocity, intima-media thickness, or arterial calcification, remains limited [2]. Therefore, there is a strong need for novel screening biomarkers to improve risk prediction.

The common carotid artery (CCA) has been extensively analyzed using B-mode ultrasound (US) imaging [3]. The deformation of the tissues in the direction parallel to the blood flow during the cardiac cycle has gained interest during the last decade [4], [5], [6], [7], [8], [9], [10], [11]. Such cyclic shearing motion of the intima-media complex with respect to the tunica adventitia, hereafter referred to as “*longitudinal kinetics*” (LOKI), has been reported to reflect vascular health [12], [13], [14], [15], [16], and may therefore constitute a valuable image-based biomarker for improved cardiovascular risk prediction.

Accurate *in vivo* quantification of LOKI in routinely acquired data is hindered by various factors, namely speckle decorrelation, out-of-plane motions, poor echogenicity, or tissue deformation. Aiming to estimate the trajectory of the

intima-media complex during US image sequences (cine-loops), a variety of motion estimation techniques have been proposed. A traditional block matching approach was used in [5], with a block of dimensions  $3.2 \times 2.5 \text{ mm}^2$ . This technique, although robust against noise, is likely to yield a precision loss due to the large dimensions of the block. Conversely, an echo tracking approach was proposed in [6], with a block of dimensions  $0.1 \times 0.1 \text{ mm}^2$ . The wall motion could be observed with a great accuracy, however this technique is more sensitive to noise, and therefore more prone to error in clinical data. A contrast optimization scheme was introduced in [10], to offer a better trade-off between noise robustness and tracking accuracy. Recent approaches have incorporated the temporal dimension into the estimation process: a Kalman filtering framework dedicated to avoid tracking divergence was proposed in [11], and a finite impulse response filtering able to handle changes in the appearance of motion targets was introduced in [16]. Nevertheless, all of these proposed techniques perform the motion estimation using the information provided by a subset of frames only (*i.e.* one or several previous frames, and the current one), and provide a solution corresponding to a succession of local optima. Instead, it could be more efficient to determine the optimal trajectory once all frames have been processed.

Dynamic programming [18], [19] is an efficient approach in combinatorial analysis, as the optimal solution among all possible combinations is determined without a costly full search. Dynamic programming has numerous applications in biomedical imaging, from tracking the motion of cells in fluorescence microscopy [20], to segmenting the contours of the intima-media complex of the CCA in B-mode US [21].

The aim of this study is to present a tracking framework based on a dynamic programming scheme, to fully incorporate the temporal dimension into the estimation process. In this approach, the cine-loop is considered as a two-dimensional plus time (2D+t) volume, in a similar fashion as previous work in the field of image registration [17]. Our rationale is to avoid tracking errors that can be locally provoked by the presence of noise or artifacts at some given time steps. The major contribution of this work is the research of a global optimum, as the resulting trajectory of the tracked point is determined *a posteriori* after all frames have been processed.

<sup>1</sup>Biomedical Imaging Group Rotterdam, Departments of Radiology and Medical Informatics, Erasmus MC, Rotterdam, The Netherlands  
g.zahnd@erasmusmc.nl

<sup>2</sup>CREATIS; CNRS UMR 5220; INSERM U1044; INSA-Lyon; Université Lyon 1; Université de Lyon; Lyon, France

<sup>3</sup>Department of Applied Mathematics and Analysis, University of Barcelona, Barcelona, Spain

<sup>4</sup>Computer Vision Center, Barcelona, Spain

<sup>5</sup>Department of Radiology, Louis Pradel Hospital, Lyon, France

<sup>6</sup>Department of Endocrinology, Louis Pradel Hospital, Hospices Civils de Lyon, Université Lyon 1, Lyon, France

<sup>7</sup>INSERM UMR 1060, Lyon, France

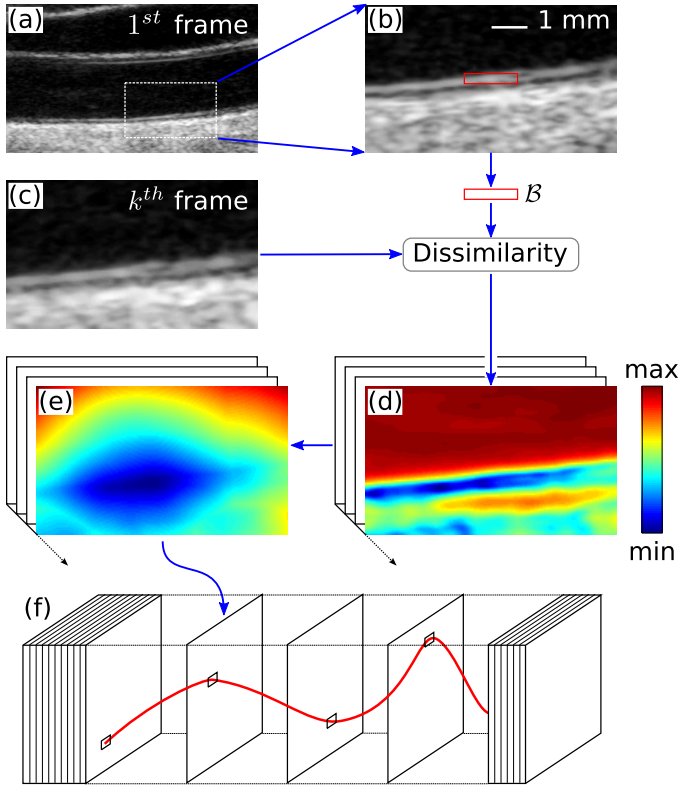


Fig. 1. Schematic representation of the motion tracking framework. (a) Common carotid artery in B-mode ultrasound imaging ( $1^{st}$  frame of the cine-loop). (b) Detailed region of the far wall. The tracked block  $\mathcal{B}$  is represented by the red rectangle within the intima-media complex. (c)  $k^{th}$  frame of the cine-loop (d) Corresponding cost function  $\mathcal{C}$ . (e) Cumulated cost function  $\mathcal{C}$ . (f) Schematic representation of the trajectory extracted from  $\mathcal{C}$  after all frames have been processed.

## II. METHODS

### A. Motion tracking

We introduce here our motion tracking framework. Since the cine-loop is considered as a 2D+t stack of frames, each point is described by three coordinates: temporal ( $k$ ), longitudinal ( $x$ ), and radial ( $y$ ). Our approach is based on four main steps, as described below.

1) *Initialization*: First, the point  $p = (1, p_x, p_y)$  to be tracked is manually selected within the intima-media complex, in the first frame of the cine-loop. The selection criteria are the following: the point should correspond to a bright echo scatterer that is well contrasted with its surroundings and remains perceptible during the entire cine-loop (Fig. 1b) [6], [11]. Centered on the initial point, a block  $\mathcal{B}$  of dimensions  $[\mathcal{B}_x, \mathcal{B}_y]$  is extracted and stored as a reference pattern. After this initial operation, the tracking is automatically carried out, as described below.

2) *Cost computation*: A 2D+t cost function  $\mathcal{C}$  is then generated, by computing the dissimilarity between the initial pattern  $\mathcal{B}$  and all the patterns corresponding to each point location in each frame of the cine-loop (Fig. 1d). Dissimilarity is computed by means of the sum of squared differences. In this function  $\mathcal{C}$ , regions likely to correspond to the actual

trajectory of the tracked point have a lower cost, as their speckle pattern is similar to the reference pattern.

3) *Dynamic programming*: From the first frame forwards, a cumulated cost map  $\mathcal{C}$  is generated *via* dynamic programming [18], [19] using a front propagation scheme (Fig. 1e). The values of  $\mathcal{C}$  corresponding to the first frame ( $k = 1$ ) are initialized according to Equation 1.

$$\begin{cases} \mathcal{C}(1, x, y) = 0, & \text{for } [x, y] = [p_x, p_y] \\ \mathcal{C}(1, x, y) = \infty, & \text{for } [x, y] \neq [p_x, p_y] \end{cases} \quad (1)$$

For  $k > 1$ , the map  $\mathcal{C}$  is iteratively generated using the relation described in Equation 2:

$$\mathcal{C}(k, x, y) = \min_{dx, dy} \left\{ \mathcal{C}(k-1, x+dx, y+dy) + \mathcal{C}(k, x, y) \cdot \sqrt{1 + \kappa_x \cdot dx^2 + \kappa_y \cdot dy^2} \right\}, \quad (2)$$

with,  $dx \in \{-\frac{N_x}{2}, \dots, 0, \dots, \frac{N_x}{2}\}$ ,  $dy \in \{-\frac{N_y}{2}, \dots, 0, \dots, \frac{N_y}{2}\}$ ,  $N_x$  and  $N_y$  being the number of reachable neighbors in the longitudinal and radial directions, respectively, and  $\kappa_x$  and  $\kappa_y$  the smoothness factor in the longitudinal and radial directions, respectively.

4) *Back-tracking*: Finally, the trajectory of the tracked point is extracted. In the last frame of the cine-loop, the point  $p'$  with the minimal cumulated cost is determined, and the optimal path is found by back-tracking the decreasing values in  $\mathcal{C}$ , from  $p'$  to  $p$ .

### B. Data acquisition

Our method was evaluated on 15 healthy volunteers (4 males, mean age  $50 \pm 3$  y.o.). B-mode US cine-loops of the left CCA (duration of at least 2 cardiac cycles) were acquired by an expert physician, using a clinical scanner (Antares, Siemens, Erlangen, Germany) with a linear probe of central frequency 8 MHz. The pixel dimensions were  $30 \times 30 \mu\text{m}$ , and the frame rate was 26 fps. The average number of frames per cine-loop was  $145 \pm 19$ .

### C. Performance evaluation

Each resulting trajectory was compared to the corresponding reference trajectory, previously constructed by three experts performing the manual tracking of the same point [11]. The tracking error was defined as the average absolute difference between the estimated trajectory and the reference trajectory, for both longitudinal and radial trajectory components.

### D. Parameter settings

Our method was applied on all cine-loops with the following parameter settings: block dimension  $\mathcal{B}_x \times \mathcal{B}_y = 1.50 \times 0.30 \text{ mm}^2$ ; smoothness constraint  $[\kappa_x, \kappa_y] = [1, 1]$ ; number of reachable neighbors  $[N_x, N_y] = [33, 33]$ , corresponding to 1 mm in both longitudinal and radial directions. The values  $\mathcal{B}_x$ ,  $\mathcal{B}_y$ ,  $N_x$  and  $N_y$  have been determined from previous work [11]. The values  $\kappa_x$  and  $\kappa_y$  have been heuristically determined.

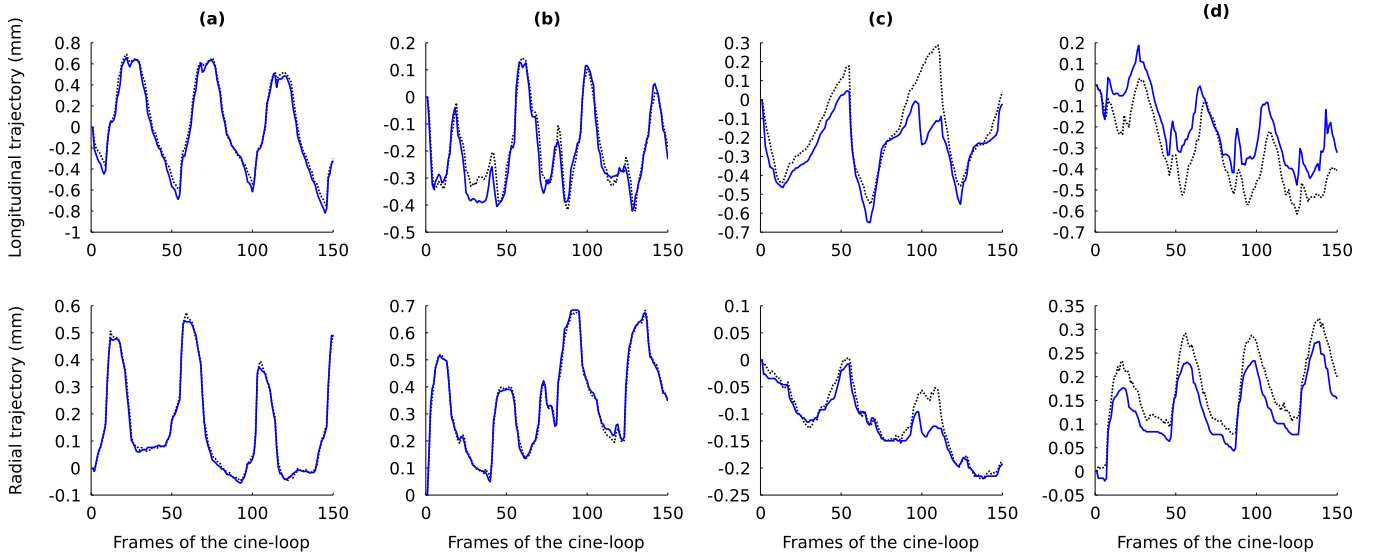


Fig. 2. Representative results of the longitudinal (first row) and radial (second row) components of the estimated trajectories (solid blue), compared with the reference trajectories (dotted black). (a,b) Successful estimations. (c) Our method fails to capture the entire amplitude of the second cycle, probably due to a large tissue motion. However, the correct trajectory is then successfully recovered thanks to the research of a global *a posteriori* optimum. (d) The estimated trajectory is similar to the reference, but the presence of a constant shift indicates that a distant point has been tracked instead of the initially selected one. This is probably due to the fact that the initial pattern was not sufficiently discriminative.

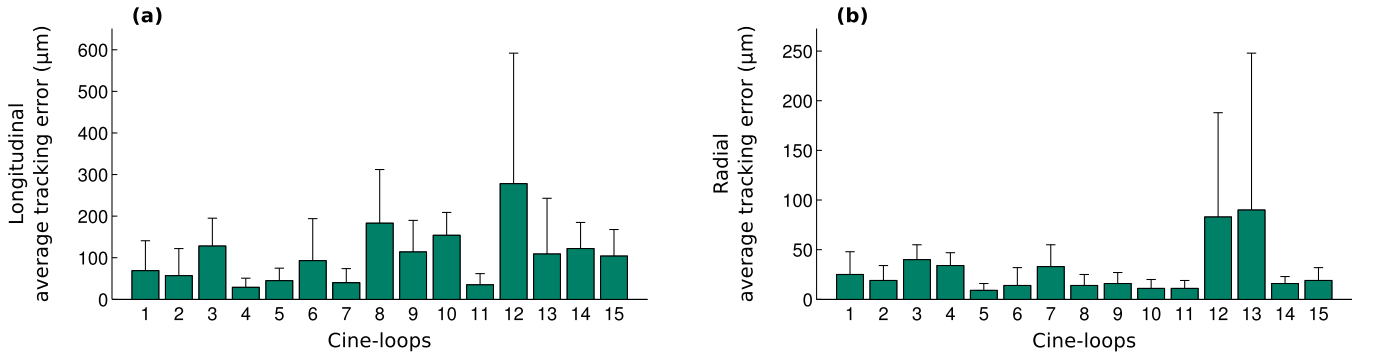


Fig. 3. Average tracking error for each cine-loop, in the longitudinal (a) and radial (b) directions. It is clearly visible that the errors are lower in the radial direction. This can be explained by the fact that the radial profile of the image presents stronger edges (*i.e.* lumen-intima and intima-media anatomical interfaces), whereas the longitudinal profile is more homogeneous.

### III. RESULTS

Representative examples of the resulting trajectories are displayed in Figure 2. The average absolute tracking errors were  $104 \pm 127 \mu\text{m}$  and  $29 \pm 57 \mu\text{m}$ , in the longitudinal and radial directions, respectively. This accuracy level is similar to the one of state-of-the-art methods [11]. The average tracking errors for each cine-loop are displayed in Figure 3.

These errors are also to be compared with the average peak-to-peak amplitude of the tissue motion, which was  $609 \pm 274 \mu\text{m}$  and  $350 \pm 320 \mu\text{m}$ , in the longitudinal and radial directions, respectively. Accordingly, the tracking error corresponded roughly to 17% and 8% of the total motion amplitude, in the longitudinal and radial directions, respectively.

Implemented in Matlab (MATLAB 7.13, The MathWorks 85 Inc., Natick, MA, USA, 2011), our method required, on average, 57 s to process a given cine-loop.

### IV. DISCUSSION

A motion tracking method was proposed to assess the trajectory of a point located in the intima-media complex of the arterial wall in B-mode US imaging. The principal characteristic of this framework is the global evaluation of an optimal trajectory after all frames of the cine-loop have been processed. Under the context of a dynamic programming approach, we proposed a front-propagation scheme adapted from the fast-marching methodology [18], [19].

In this work, the parameter settings have been determined heuristically. As the smoothness constraint terms  $\kappa_x$  and  $\kappa_y$  are used to penalize abrupt displacements, it is likely that the values used here would be sub-optimal when applied to a different dataset where the tissue motion is different (*i.e.* either due to the frame rate of the sonograph, or to stiffer arteries in patients). A thorough evaluation of the actual impact of the parameter settings in a larger dataset,

including diseased participants, is thus required in further studies.

The major drawback of this framework is the assumption that the tracked pattern remains similar during the entire length of the cine-loop. Actually, the initial pattern of the block  $B$  selected in the first frame is used to generate the  $2D+t$  cost function  $C$ . As moving tissues may undergo a shearing deformation during the heart beat, the appearance of the corresponding pattern is likely to vary. Therefore, an adaptive reference pattern would probably be better tailored to keep track of the moving point. This issue will be tackled in future work.

In conclusion, fully incorporating the temporal dimension into the estimation process by considering the set of frames as a  $2D+t$  volume could constitute a promising approach for improved estimation of the arterial wall motion in US imaging.

#### ACKNOWLEDGMENT

This work was done within the French ANR LABEX PRIMES (ANR-11-LABX-0063) and CeLyA (ANR-10-LABX-0060) of Université de Lyon, within the program “Investissements d’Avenir” (ANR-11-IDEX-0007) operated by the French National Research Agency (ANR).

#### REFERENCES

- [1] World Health Organization, Cardiovascular diseases (CVDs), Fact sheet number 317, March 2013, <http://www.who.int/mediacentre/factsheets/fs317/en/index.html>.
- [2] A. Simon, G. Chironi, and J. Levenson, Performance of subclinical arterial disease detection as a screening test for coronary heart disease, *Hypertension*, vol. 48, no. 3, pp. 392–396, 2006.
- [3] S. Golemati, A. Gastounioti, and K. S. Nikita, Toward novel noninvasive and low-cost markers for predicting strokes in asymptomatic carotid atherosclerosis: The role of ultrasound image analysis, *IEEE Transactions on Biomedical Engineering*, vol. 60, no. 3, pp. 652–658, 2013.
- [4] M. Persson, Å. R. Ahlgren, T. Jansson, A. Eriksson, H. W. Persson, K. Lindström, A new non-invasive ultrasonic method for simultaneous measurements of longitudinal and radial arterial wall movements: First in vivo trial, *Clinical Physiology and Functional Imaging*, vol. 23, pp. 247–251, 2003.
- [5] S. Golemati, A. Sassano, M. Lever, A. Bharath, S. Dhanjil, and A. Nicolaides, Carotid artery wall motion estimated from B-mode ultrasound using region tracking and block matching, *Ultrasound in Medicine & Biology*, vol. 29, no. 3, pp. 387–399, 2003.
- [6] M. Cinthio, Å. R. Ahlgren, T. Jansson, A. Eriksson, H. W. Persson, and K. Lindström, Evaluation of an ultrasonic echo-tracking method for measurements of arterial wall movements in two dimensions, *IEEE Transactions on Ultrasonics, Ferroelectrics and Frequency Control*, vol. 52, pp. 1300–1311, 2005.
- [7] M. Cinthio, Å. R. Ahlgren, J. Bergkvist, T. Jansson, H. W. Persson, and K. Lindström, Longitudinal movements and resulting shear strain of the arterial wall, *Am J Physiol*, vol. 291, no. 1, pp. H394–H402, 2006.
- [8] T. Idzenga, S. Holewijn, H. H. G. Hansen, and C. L. de Korte, Estimating cyclic shear strain in the common carotid artery using radiofrequency ultrasound, *Ultrasound in Medicine & Biology*, vol. 38, pp. 2229–2237, 2012.
- [9] E. Soleimani, M. Mokhtari Dizaji, and H. Saberi, Carotid artery wall motion estimation from consecutive ultrasonic images: Comparison between block-matching and maximum-gradient algorithms, *J Teh Univ Heart Ctr*, vol. 6, no. 2, pp. 72–78, 2012.
- [10] H. Yli-Ollila, T. Laitinen, M. Weckström, and T. M. Laitinen, Axial and radial waveforms in common carotid artery: An advanced method for studying arterial elastic properties in ultrasound imaging, *Ultrasound in Medicine & Biology*, vol. 39, no. 7, pp. 1168–1177, 2013.
- [11] G. Zahnd, M. Orkisz, A. Sérusclat, P. Moulin, and D. Vray, Evaluation of a Kalman-based block matching method to assess the bi-dimensional motion of the carotid artery wall in B-mode ultrasound sequences, *Medical Image Analysis*, vol. 17, no. 5, pp. 573–585, 2013.
- [12] S. Svedlund, C. Eklund, P. Robertsson, M. Lomsky, and L. M. Gan, Carotid artery longitudinal displacement predicts 1-year cardiovascular outcome in patients with suspected coronary artery disease, *Arterioscler Thromb Vasc Biol*, vol. 31, pp. 1668–1674, 2011.
- [13] G. Zahnd, L. Boussel, A. Marion, M. Durand, P. Moulin, A. Sérusclat, and D. Vray, Measurement of two-dimensional movement parameters of the carotid artery wall for early detection of arteriosclerosis: A preliminary clinical study, *Ultrasound in Medicine & Biology*, vol. 37, no. 9, pp. 1421–1429, 2011.
- [14] G. Zahnd, D. Vray, A. Sérusclat, D. Alibay, M. Bartold, A. Brown, M. Durand, L. M. Jamieson, K. Kapellas, L. J. Maple-Brown, K. O’Dea, P. Moulin, D. S. Celermajer, and M. R. Skilton, Longitudinal displacement of the carotid wall and cardiovascular risk factors: associations with aging, adiposity, blood pressure and periodontal disease independent of cross-sectional distensibility and intima-media thickness, *Ultrasound in Medicine & Biology*, vol. 38, no. 10, pp. 1705–1715, 2012.
- [15] Å. R. Ahlgren, M. Cinthio, S. Steen, T. Nilsson, T. Sjöberg, H. W. Persson, and K. Lindström, Longitudinal displacement and intramural shear strain of the porcine carotid artery undergo profound changes in response to catecholamines, *Am J Physiol – Heart and Circulatory Physiology*, vol. 302, no. 5, pp. H1102–H1115, 2012.
- [16] A. Gastounioti, S. Golemati, J. S. Stoitsis, and K. S. Nikita, Carotid artery wall motion analysis from B-mode ultrasound using adaptive block matching: in silico evaluation and in vivo application, *Physics in Medicine and Biology*, vol. 58, no. 24, pp. 8647, 2013.
- [17] C. T. Metz, S. Klein, M. Schaap, T. van Walsum, and W. Niessen, Nonrigid registration of dynamic medical imaging data using nD+t B-splines and a groupwise optimization approach, *Medical Image Analysis*, vol. 15, no. 2, pp. 238–249, 2011.
- [18] J. A. Sethian, A fast marching level set method for monotonically advancing fronts, *Proc Natl Acad Sci*, vol. 93, no. 4, pp. 1591–1595, 1996.
- [19] L. Cohen, Minimal paths and fast marching methods for image analysis, In: N. Paragios, Y. Chen, O. Faugeras (Eds), *Handbook of mathematical models in computer vision*, Springer, US, 97–111, 2006.
- [20] D. Padfield, J. Rittscher, N. Thomas, and B. Roysam, Spatio-temporal cell cycle phase analysis using level sets and fast marching methods, *Medical Image Analysis*, vol. 13, no. 1, pp. 143–155, 2009.
- [21] G. Zahnd, M. Orkisz, A. Sérusclat, P. Moulin, and D. Vray, Simultaneous extraction of carotid artery intima-media interfaces in ultrasound images: Assessment of wall thickness temporal variation during the cardiac cycle, *Int J CARS*, DOI: 10.1007/s11548-013-0945-0, in press (2013).